

# A New Performance Regime for Microfabricated Ball Bearings

**Brendan Hanrahan<sup>1,2\*</sup>, Mustafa Beyaz<sup>3</sup>, Matthew McCarthy<sup>4</sup>, C. Mike Waits<sup>2</sup>, and Reza Ghodssi<sup>3</sup>**

<sup>1</sup>Dept. of Materials Science and Engineering, University of Maryland, College Park, MD 20742, USA

<sup>2</sup>The US Army Research Laboratory, Adelphi, MD 20783, USA

<sup>3</sup>Dept. of Electrical and Computer Engineering, Institute for Systems Research, University of Maryland, College Park, MD 20742, USA

<sup>4</sup>Mechanical Engineering Department, Drexel University, Philadelphia, PA 19104, USA

\*Presenting author: bhanrah@umd.edu

**Abstract:** This work presents a study of the fundamental tribological mechanisms dictating the performance of microfabricated silicon/steel bearing systems, serving as the mechanical contact for current and future micro-power and –energy devices. Silicon thrust bearings packed with stainless steel balls have been operated up to 200mN normal force for over 20M revolutions without performance degradation. Amorphization of silicon raceways and steel ball material adhesion were determined to be the primary wear mechanisms within microfabricated raceways. Additionally, a relationship between friction torque and applied load is derived from Hertzian contact mechanics and validated by experiments. The experimentally derived relationship leads to a greater understanding of the tribology of micro-scale rolling contacts and the impact on future microsystems.

**Keywords:** tribology, friction, microturbine, microball bearing

## INTRODUCTION

Progress in microfabricated ball bearing technology has led to the realization of functional rotary Micro-ElectroMechanical Systems (MEMS). Microball bearings have been demonstrated to be a viable mechanical support in micromotors and micropumps [1,2] with applications in power and energy conversion. To date, demonstration of these devices has been limited to relatively low lifetimes and loads, due to the lack of understanding of the fundamental tribology of the micro-scale rolling contacts.

The tribological phenomena observed in microfabricated systems differ significantly from macro-scale counterparts. This is due to an increased surface-to-volume ratio obtained from scaling features to shorter length scales and the non-ideal materials for mechanical/tribological applications used in silicon-based microfabrication techniques. Several studies utilized atomic force microscopy or friction force microscopy to characterize system level friction [3,4], studying the effect of sliding velocity on adhesion and friction force. A majority of these studies are focused on sliding or static regime friction on micro and continuum length scales, with limited work on the unique realm of microscale rolling friction.

Ghodssi, *et al.*, first characterized the static friction in microball bearing supported linear actuator [5]. This work studied the interaction between stainless steel microballs and different micromachined materials systems. From here, the research of Lin, *et al.*, [6] modeled the friction of various configurations

of a microball supported linear actuator, with special attention paid to the effects of speed and load. Lin found COF values between 0.007 and 0.015 if there is no ball-on-ball contact in a free sliding linear bearing. Tan expanded on the empirical work in [5,6] and created a viscous model for a steel ball rolling on a silicon plane and predicted COF of 0.007 for speeds  $\pm 0.2$  m/s [7]. McCarthy *et al.* hypothesized that the friction in the linear bearing from [7] was directly related to the contact area [8]. McCarthy then developed an empirical power-law relationship to describe the observed Dynamic Friction torque/load relationship in a high speed rotary system. This work found a velocity dependant coefficient of friction from X-Y at normal loads from 5-50mN [9].

Limited work has been performed to understand the tribology that ultimately dictates the performance and lifetime of silicon microfabricated rolling bearings. This study aims to illuminate the tribological processes dictating the long-term performance of microball bearing systems.

## EXPERIMENT

### Microturbine Design

The microfabricated silicon test device (MTD) is shown in figure 1. The MTD consists of a through-hole etched plumbing chip used to direct actuation flow, aligned to a set of eutectically bonded wafers containing the thrust-side release etch and turbine actuation structures.

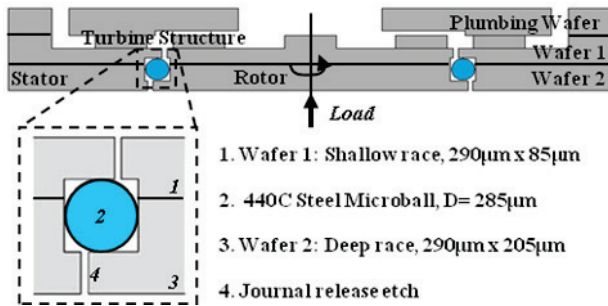


Figure 1 Cross section schematic of the microturbine tribology test device with a close-up of the raceway.

The microballs are encapsulated by two bonded silicon layers with a raceway DRIE into each layer. The raceway is designed to allow for 5  $\mu\text{m}$  of radial play, chosen to mitigate ball jamming while allowing for reasonable bond tolerances. The bearing exhibits no play in the thrust direction because of the normal force on the rotor. The bearing depths are asymmetrically etched such that one bearing is designed to be 190  $\mu\text{m}$  deep and the other 90  $\mu\text{m}$ , resulting in less than 10 nm average surface roughness, typical for DRIE etched structures. The purpose of the offset etch depths is preventing the ball from contacting the bond interface during operation.

A journal is etched completely through each wafer to create a rotor that is supported only by the microball bearings. After bonding, turbine blades and vanes are etched into the top die with a height of 250  $\mu\text{m}$ , simultaneously reaching the journal etch and releasing the turbine side of the device. Similarly, the thrust-side release structure is etched into the backside of the bonded test device, completely releasing the rotor. A complete fabrication schematic of the bearings can be found in [1]. One important feature of the packaging of the test device is allowing for turbine flow and a thrust plenum to be operated independently, decoupling of thrust and actuation loads as described in [9].

### Testing Methodology

Friction torque measurements were obtained for each test device at normal loads ranging from 10-200 mN. To begin, the thrust plenum pressure is set to provide a prescribed normal load to the bearings. The independent turbine flow then actuates the released rotor structure via the deep-etched turbine blades and vanes. After the turbine has equilibrated to a steady rotational speed, the actuation flow is cut-off and the turbine is left to decelerate under only the pressure of the thrust plenum. Friction torque over the speed range of 1,000-10,000 rpm, or dynamic friction torque (DFT), is obtained from the second derivative of a power law fit to the position data from the spin-down. Upon conclusion of spin-down tests, the MTD is

actuated for 5 million revolutions (Mrevs) increments up to 20Mrevs under a constant normal load, in this case 10mN or 200mN at speeds below 10,000 rpm.

Turbine operation curves are utilized to characterize the system-level operation of the turbine at progressive lifetimes to determine the general performance of the device. For these tests, rotation speed was measured as a function of input power provided by the turbine flow. The initial test is taken after a brief run-in period to remove any acute fabrication defects in the raceway. It is expected that minute changes in performance properties will be over-powered by the driving flow.

## DISCUSSION

### Long-term Performance

Turbine performance curves are utilized to determine the global performance of the system. During testing the turbine is actuated by compressed nitrogen and the speed and input power are measured. Figure 2 shows performance curves taken after run-in and after 20Mrevs of operation for a MTD actuated under a constant load of 200mN.

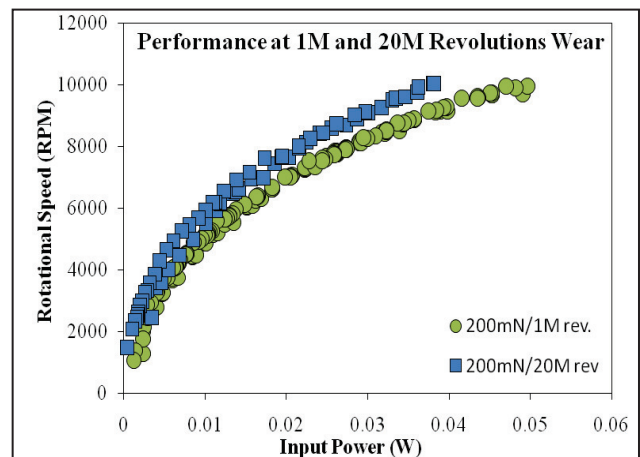


Figure 2 Performance comparison for a MTD tested under 200mN normal loads at 1Mrev. and 20Mrev. running time .

The performance of the highest loaded turbine exhibits improved operation over the duration of testing. The improvement can be observed as a 20% decrease in power needed to achieve 10,000 rpm after extended testing. The increased turbine efficiency is a product of the run-in properties of the silicon raceways, mostly the smoothing of raceway asperities and removal of extraneous material from the journals. It should be noted that the tested turbines have not yet reached critical failure and are still under test.

### Wear

Surface analysis techniques are utilized to determine the wear mechanisms of the long-lived

systems. In previous work [1-2,9], silicon fracture at the high-stress contact points was the primary wear mechanism. The asymmetric raceway design (figure 1 *inset*) pioneered in [1] removes high-stress contacts and allows for extended operation into previously unknown wear regimes. This study utilized Electron Dispersive X-Ray Analysis (EDS) and Raman spectroscopy to chemically analyze the raceways within the ball contact area.

Figure 3 shows Raman spectra taken from two raceways under different levels of load and operation time.

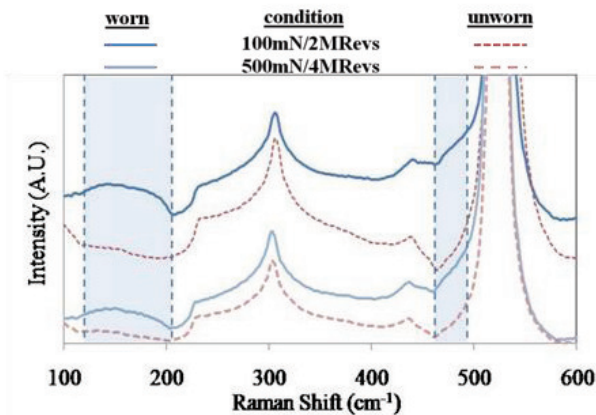


Figure 3 Raman Spectra from two silicon raceways with different contact pressures and lifetimes.

The broad peak at  $160\text{ cm}^{-1}$  and the shoulder at  $470\text{ cm}^{-1}$  coincide with a stress-induced amorphous-silicon ( $\alpha$ -Si) phase specific to the worn areas of the race. The significant at  $520\text{ cm}^{-1}$  is representative of the single crystalline silicon background. Nanoindentation studies on silicon [10] have shown that pressure induced phase transformations occur with contact pressures less than 4.5 GPa. The rotor load was measured at 100mN and 500mN for the spectra shown above, corresponding to a minimum contact pressure of 440 MPa and 750 MPa, respectively. The calculated contact pressure is assumed to be an underestimate because etch variations in raceway depth could provide conditions where certain balls are supporting a higher proportion of the rotor load. It is difficult to draw a direct reference between the nanoindentation studies and the results presented within due to the dramatically faster loading and unloading rates and number of cycles imparted by the rotating microballs. This work illuminates the presence of an  $\alpha$ -Si phase, which exhibits fracture toughness values increased over silicon that may help to mitigate further wear.

The second source of wear in the microfabricated bearing was found to be adhesion of ball material on the raceway. This is observed physically with scanning electron microscopy and chemically using

an adjoining EDS analysis. The results shown in figure 4 illuminate the presences of iron and chromium peaks in the EDS spectra, which is adhered ball material.

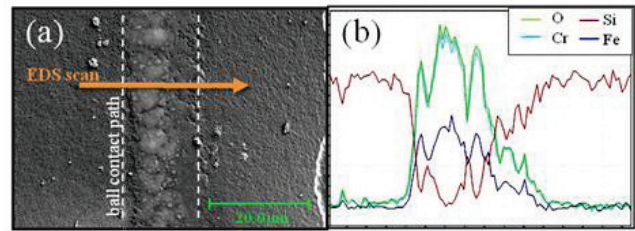


Figure 4 (a) Scanning Electron Microscope images of characteristic wear for silicon, raceways. EDS line scans taken perpendicular to the wear track presented in (b), correlating with the adjacent SEM image.

Ball adhesion to the raceways arises from chemical bonding that occurs during a high-pressure contact event when a ball contacts a raceway asperity. As the ball continues to roll, the lowest energy path is taken potentially resulting crack propagation mechanism through the surface of the ball rather than at the newly-formed bond interface. Cumulatively this process isn't expected to be self-limiting and could prove to be an ultimate failure mechanism of the microfabricated bearings.

### Friction Torque

The relationship between DFT and normal load is improved in this study from work presented at *PowerMEMS'09*. The previous study [11] of friction torque were based on a load range of 10-50 mN and a linear relationship with normal load was found of the form (eq. 1):

$$DFT = aL + b \quad (1)$$

Testing a broader range of loads, from 5 to 100 mN, reveals a  $Load^{2/3}$  dependence of friction torque on normal load while maintaining the load-independent constant  $b$  from the previous work (eq. 2):

$$DFT = aL^{2/3} + b \quad (2)$$

The load-independent constant is expected to contain contributions to friction torque that are primarily due to variations in speed of the turbine, such as gyroscopic forces, viscous drag in the journal bearings, and vibration in the bearing. Figure 5 compares the spin-down obtained DFT data presented in [11] with the new DFT data for a higher-load-range turbine.

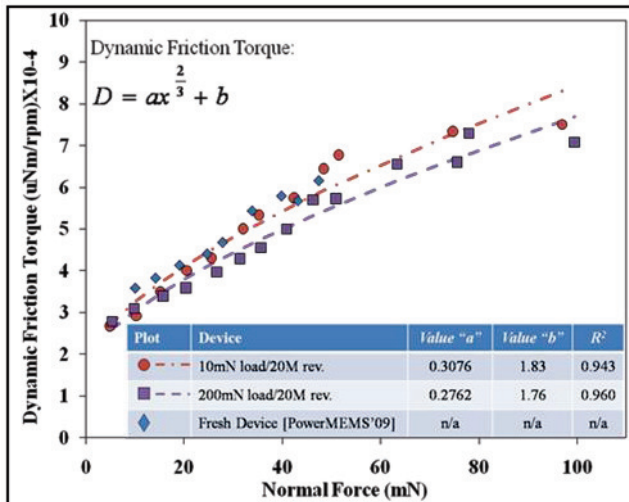


**Figure 5** The results of spin-down friction testing of devices after 20Mrev. wear compared with a previously reported silicon turbine[11].

The updated DFT relationship in a microfabricated bearing is significantly different from the relationship observed in macroscale systems, typically reported to be  $DFT \propto Load^{\frac{4}{3}}$  in pure thrust bearings, which can be derived from the effect of volumetric hysteresis on friction. The microfabricated systems have a greater surface-to-volume ratio, so it is expected that surface effects will dictate system level friction. Accordingly, the new relationship has been derived from the formula for the contact area of a sphere on a flat plane from Hertzian contact mechanics and corresponds well to the geometries obtained in microfabricated bearings. By relating fundamental contact areas and observed friction phenomena, the influence of surface area is observed on measured friction within the microfabricated bearing.

## CONCLUSION

Silicon microfabricated bearings with steel balls are investigated to loads and lifetimes previously unexplored, demonstrating the robustness of microball bearing supports for future MEMS platforms. The long-term wear mechanisms of surface amorphization and ball adhesion are found to be the primary wear mechanisms for long-lived devices. A relationship between friction torque and applied load is derived from Hertzian contact mechanics and validated by experiments. The experimentally derived relationship suggests that surface effects dominate over volumetric contributions to rolling friction, unique to the micro-rolling regime.

## ACKNOWLEDGEMENTS:

The authors would like to acknowledge the US Army

Research Laboratory Cleanroom and Maryland Nanocenter.

## REFERENCES

- [1] C. Mike Waits, M. McCarthy, and R. Ghodssi, 2010 A Microfabricated Spiral-Groove Turbopump Supported on Microball Bearings *JMEMS* 19 1 99-109
- [2] M. McCarthy, C. M. Waits, M. I. Beyaz, and R. Ghodssi, 2009 A Rotary Microactuator Supported on Encapsulated Microball Bearings Using an Electro-pneumatic Thrust Balance *JMM* 19 9 1-7
- [3] N. S. Tambe and B. Bhushan, 2005 Nanowear mapping: A novel atomic force microscopy based approach for studying nanoscale wear at high sliding velocities *Trib. Let.* **20** 83-90
- [4] B. Bhushan 1998 Micro/nanotribology using atomic force microscopy/friction force microscopy: state of the art *Proc. Inst. Mech. Eng. J Eng. Trib.* **212** 1-18
- [5] R. Ghodssi, D. D. Denton, A. A. Seireg, and B. Howland, 1993 Rolling Friction In A Linear Microactuator *J. Vac. Sci. & Tech. A* **11** 803-807
- [6] T. W. Lin, A. Modafe, B. Shapiro, and R. Ghodssi, 2004 Characterization of dynamic friction in MEMS-Based microball bearings *IEEE Trans. Inst. & Meas.* **53** 839-846
- [7] X. B. Tan, A. Modafe, and R. Ghodssi, 2006 Measurement and modeling of dynamic rolling friction in linear microball bearings *J. Of Dyn. Sys. Meas. & Cont.-Trans. ASME* **128** 891-898
- [8] M. McCarthy, B. Hanrahan, C. Zorman, and R. Ghodssi, 2007 Rolling Friction in MEMS Ball Bearings: The Effects of Loading and Solid Film Lubrication," *STLE/ASME Int'natl Joint Trib. Conf., San Diego, CA, October 22 - 24*
- [9] M. McCarthy, C. M. Waits, and R. Ghodssi, 2009 Dynamic Friction and Wear in a Planar-Contact Encapsulated Microball Bearing using an Integrated Microturbine *JMEMS* **18** 2 263-273
- [10] V. Domnich, Y. Gogotsi, and S. Dub 2000 Effect of phase transformations on the shape of the unloading curve in the nanoindentation of silicon," *App. Phys. Let.* **76** 2214-2216
- [11] B. Hanrahan, M. McCarthy, J. Balsam, C.M. Waits, H. Bruck, and R. Ghodssi, 2009 Hard Film Coatings for High-Speed Rotary MEMS Supported on Microball Bearings *PowerMEMS 2009 (Washington, DC, December 1-4, 2009)* 589-592